Detection of Conformational Changes in Actin by Fluorescence Resonance Energy Transfer between Tyrosine-69 and Cysteine-374†

Masao Miki

Muscle Research Unit, Department of Anatomy, The University of Sydney, Sydney, New South Wales 2006, Australia

Received June 11, 1991; Revised Manuscript Received August 22, 1991

ABSTRACT: The distance between 5-(dimethylamino)naphthalene-1-sulfonyl chloride (dansyl chloride or DNS-Cl) attached to Tyr-69 and *N*-[4-[[4-(dimethylamino)phenyl]azo]phenyl]maleimide (DABMI) or *N*-[4-(dimethylamino)-3,5-dinitrophenyl]maleimide (DDPM) attached to Cys-374 in an actin monomer was measured to be 2.51 nm or 2.27 ± 0.04 nm, respectively, by fluorescence resonance energy transfer. This distance does not change significantly when the actin monomer binds DNase I, when the monomer is polymerized, when the polymer interacts with myosin subfragment 1, or when it interacts with tropomyosin–troponin in the presence and absence of Ca^{2+}. Changes in the distance were within 0.1 nm. The results indicate that the structure of the region involving Tyr-69 and Cys-374 is substantially rigid. A large blue shift (about 15 nm) of the fluorescence spectrum and a large increase (about 80%) in the fluorescence intensity of DNS-actin were observed when DNS-actin was denatured upon addition of EDTA. On the other hand, a red shift (about 7 nm) of the fluorescence spectrum and a large decrease (about 50%) in the fluorescence intensity were observed when DNS-actin was completely unfolded in 8 M urea. The results indicate that dansyl chromophore becomes less exposed to the aqueous environment by EDTA denaturation in contradiction to the case of intrinsic tryptophan residues in G-actin. Resonance energy transfer measurements showed that the distance between probes attached to Tyr-69 and Cys-374 on an actin monomer changes by 0.37 nm during EDTA denaturation, but that the distance becomes longer than 4.0 nm in 8 M urea in which no energy transfer is observed. The results indicate that the structure of the region involving Tyr-69 and Cys-374 is largely preserved even after the denaturation by EDTA. The addition of ATP decreases the rate of EDTA denaturation but does not inhibit it. DNase I strongly protects the actin structure from EDTA denaturation, while myosin subfragment 1 has no effect.

Actin is vital in eucaryotic cells. It interacts with many other proteins and plays essential roles not only in generating force but also in forming cytoskeleton [see reviews: Oosawa (1983) and Pollard (1990)]. Actin exists in a monomeric form (G-actin) at low ionic strength, and in a filamentous form (F-actin) under physiological conditions. One mole of actin binds 1 mol of both ATP (or ADP) and Ca^{2+}. The atomic structure of actin has been recently revealed by X-ray crystallography at 0.3-nm resolution in the complex form with DNase I (Kabsch et al., 1990). According to this model, actin consists of two well-separated domains which are further subdivided into two subdomains. Subdomains 1 and 2 constitute the small domain, whereas subdomains 3 and 4 comprise the large domain. The nucleotide is located at the cleft region with a calcium ion bound to the β-phosphate. An atomic model of F-actin can also be constructed to fit the observed X-ray diagram from oriented gels of F-actin, using the atomic model of the actin monomer (Holmes et al., 1990). This F-actin model is based on the assumption that the structure of the actin monomer in F-actin is not significantly different from that in the cocrystals. However, in solution, actin may adopt different conformations in response to its states (i.e., the complex with DNase I, G-actin, F-actin, etc.). Therefore, it is important to study whether or not there is a difference between the structures in these states. Fluorescence resonance energy transfer has been extensively used for studying the spatial relationships between residues on muscle proteins [see reviews: Botts et al. (1984) and dos Remedios et al. (1988)]. This method is especially valuable for detecting a small conformational change, since the transfer efficiency is a function of the inverse of the sixth power of the distance between probes (Förster, 1948). Such determinations are beyond the scope of current X-ray diffraction analyses.

The removal of the bound metal in G-actin upon addition of EDTA induces a release of the bound ATP, and consequently G-actin rapidly loses its ability to polymerize (Maruyama & Gergely, 1961). This inactivated state of G-actin largely maintains its secondary structure and differs from the completely unfolded form in 8 M urea (Lewis et al., 1963; Lehrer & Kerwar, 1972; Strzelecka-Golaszewska et al., 1985; Kuznetsova et al., 1988). The transition from the completely unfolded form to the inactivated state is readily reversible, but the transition from native form to the inactivated state is irreversible (Lehrer & Kerwar, 1972; Kuznetsova et al., 1988). The study of this intermediate state is important for elucidation of the process of protein folding and functioning.

In the present paper, Tyr-69 is labeled with DNS-Cl[1] as the resonance energy donor while Cys-374 is labeled with DABMI or DDPM as the energy acceptor. Then, the spatial relationship between Tyr-69 and Cys-374 and also its change have been studied when G-actin forms a complex with DNase I, when it assembles into polymers (F-actin), when F-actin interacts with myosin subfragment I or tropomyosin–troponin,

† This research was supported by grants from the National Health and Medical Research Council of Australia.

[1] Abbreviations: S1, myosin subfragment 1; DABMI, *N*-[4-[[4-(dimethylamino)phenyl]azo]phenyl]maleimide; DDPM, *N*-[4-(dimethylamino)-3,5-dinitrophenyl]maleimide; dansyl chloride or DNS-Cl, 5-(dimethylamino)naphthalene-1-sulfonyl chloride; DNS-actin, actin labeled at Tyr-69 with DNS-Cl; DNS-DABM-actin, actin labeled at Tyr-69 with DNC-Cl and at Cys-374 with DABMI; DNS-DDPM-actin, actin labeled at Tyr-69 with DNS-Cl and at Cys-374 with DDPM; EGTA, ethylene glycol bis(2-aminoethyl ether)-*N*,*N*,*N*′,*N*′-tetraacetic acid.

0006-2960/91/0430-10878$02.50/0

and when G-actin is denatured upon addition of EDTA or urea. The atomic model of actin locates Tyr-69 in subdomain 2 which is in the same domain but in a different subdomain of Cys-374 (subdomain 1) (Kabsch et al., 1990). The present results indicate that the small domain of the actin monomer is substantially rigid. The spatial relationship between Tyr-69 and Cys-374 in G-actin and F-actin is in good accordance with the atomic models of actin. These results provide strong support for the atomic models of actin. Furthermore, in combination with the atomic models of actin, the present information is useful for studying a relation between the function and structure of the actin molecule.

Materials and Methods

Reagents. Phalloidin from *Amanita phalloides* was purchased from Boehringer Mannheim Biochemica. DNase I from bovine pancreas, DNA from calf thymus, and DNS-Cl were from Sigma Chemical Co. DDPM was from Aldrich Chemical Co., and DABMI was from Molecular Probes. Fractogel TSK HW 55(s) was from Merck. BCA protein assay reagent was from Pierce Chemicals. Tetranitromethane was synthesized according to the method of Liang (1941). All other chemicals were analytical grade.

Protein Preparations. Actin was prepared from acetone powder of rabbit skeletal muscle according to the method of Spudich and Watt (1971). S1 was prepared from rabbit skeletal muscle myosin by chymotryptic digestion according to the method of Weeds ad Pope (1977) and purified on a column (2.8 × 90 cm) of Fractogel TSK HW 55(s). Tropomyosin and troponin were extracted from the muscle residue after extraction of myosin and purified by the method of Ebashi et al. (1968). Protein concentrations were determined from absorbance measurements, by use of absorption coefficients of A_{290nm} = 0.63 $(mg/mL)^{-1}$ cm^{-1} for G-actin (Lehrer & Kerwar, 1973) and A_{280nm} = 0.75 $(mg/mL)^{-1}$ cm^{-1} for S1 (Weeds & Pope, 1977), 0.33 $(mg/mL)^{-1}$ cm^{-1} for tropomyosin (Cummins & Perry, 1973), and 0.45 $(mg/mL)^{-1}$ cm^{-1} for troponin (Ishiwata & Fujime, 1972). Concentrations of DNase I and labeled actin were determined with the Pierce BCA protein assay reagent by use of unlabeled actin as the standard. Relative molecular masses of 42000 for actin, 115000 for S1, 66000 for tropomyosin, 69000 for troponin, and 31000 for DNase I were used.

Labeling of Actin at Tyr-69 with DNS-Cl. Tetrathionate reacts with sulfhydryl groups of proteins to form sulfenyl thiosulfate derivatives under reversible conditions (Pihl & Lange, 1962). This reaction was used for a reversible protection of sulfhydryl groups of proteins (Kassab et al., 1968; Goto et al., 1971). Reactive thiols on G-actin were protected by the treatment with sodium tetrathionate before the nitration of Tyr-69 with tetranitromethane, since tetranitromethane reacts preferentially with thiols and forms disulfide or sulfonic acid (Riordan & Christen, 1968). G-Actin (about 3 mg/mL) was mixed with a 20-fold molar excess of sodium tetrathionate in 0.2 mM ATP/0.1 mM $CaCl_2$/1 mM Tris-HCl (pH 8.0) (buffer G) for 30 min at 4 °C followed by dialysis against buffer G. This protection of thiols did not impair the ability to polymerize. Then, Tyr-69 was modified with tetranitromethane according to the method of Chantler and Gratzer (1975) with a slight modification (Miki et al., 1987a). A 60-fold molar excess of tetranitromethane was mixed with actin in 0.5 mM ATP/0.1 mM $CaCl_2$/1 mM Tris-HCl (pH 8.0) at 4 °C, keeping the pH at 8.0. After 30 min, the reaction was terminated by the addition of an equimolar dithiothreitol over tetranitromethane, keeping the pH at 7.5 ± 0.4. The sample was exhaustively dialyzed against buffer G. The labeling ratio of tetranitromethane to actin was 1.1 as previously reported (Miki et al., 1987a). Nitrated actin was reduced to with a 50-fold molar excess of sodium dithionite followed by dialysis against buffer G. Before the reaction with DNS-Cl, reactive thiols were protected again by the treatment with sodium tetrathionate (Kassab et al., 1968), since the thiol protection was removed by the addition of dithiothreitol when the reaction with tetranitromethane was stopped. Then, the aminotyrosyl derivative was reacted with a 4-fold molar excess of DNS-Cl in 0.5 mM ATP/2 mM phosphate buffer, keeping the pH at 6.5 for 14 h at 4 °C followed by dialysis against 0.2 mM ATP/0.1 mM $CaCl_2$/2 mM phosphate buffer (pH 6.5) for removing unreacted DNS-Cl. The protection of thiol was removed again by the addition of 1 mM dithiothreitol following dialysis against buffer G. Finally, the sample solution was clarified by ultracentrifugation at 100000*g* for 1 h. Labeled actin was lyophilized in the presence of 0.1 M sucrose and kept at −20 °C. The labeling ratio of DNS-Cl to actin was determined to be 1.1, using the absorption coefficient of 4600 M^{-1} cm^{-1} at 340 nm (Kenner & Neurath, 1971).

Double Labeling at Tyr-69 and Cys-374. Actin labeled at Tyr-69 with DNS-Cl (DNS-actin) was further modified at Cys-374 with DABMI (DNS-DABM-actin) or DDPM (DNS-DDPM-actin). DNS-actin (about 1.5 mg/mL) was mixed with a 5-fold molar excess of DABMI or DDPM in 0.5 mM ATP/0.1 mM $CaCl_2$/2 mM Tris-HCl (pH 8.0) at 4 °C for 17–24 h, and the reaction was stopped by adding 1 mM 2-mercaptoethanol. The samples were dialyzed exhaustively against buffer G, clarified by centrifugation at 100000*g* for 1 h, lyophilized in 0.1 M sucrose, and kept at −20 °C in the dark. The labeling ratios of DABMI and DDPM to actin were 1.0 ± 0.05, by use of the absorption coefficients of 24800 M^{-1} cm^{-1} at 460 nm for DABMI (Tao et al., 1983) and 3050 M^{-1} cm^{-1} at 440 nm for DDPM (Gold & Segel, 1964).

Spectroscopic Measurements. Absorption was measured with a Philips PU 8800 spectrophotometer. Fluorescence was measured with an SLM 8000 spectrophotometer in the ratio mode by photon counting. Sample cells were placed in a thermostated cell holder. For fluorescence intensity measurements, exciting light was polarized at 35° in order to compensate for the effect of rotational motion of the chromophores.

Fluorescence Resonance Energy Transfer. The efficiency, E, of resonance energy transfer between probes was determined by measuring the fluorescence intensity of the donor both in the presence (F_{DA}) and in the absence (F_{D0}) of the acceptor as given by

$$E = 1 - F_{DA}/F_{D0} \quad (1)$$

The efficiency is related to the distance (R) between probes and Förster's critical distance (R_0) at which the transfer efficiency is equal to 50% by

$$E = R_0^6/(R_0^6 + R^6) \quad (2)$$

R_0 can be obtained (in nm) by

$$R_0^6 = (8.79 \times 10^{-11}) n^{-4} \kappa^2 Q_{D0} J \quad (3)$$

where n is the refractive index of the medium taken to be 1.4, κ^2 is the orientation factor, Q_{D0} is the quantum yield of the donor in the absence of the acceptor, and J is the spectral overlap integral (in M^{-1} cm^{-1} nm^4) between the donor emission $F_D(\lambda)$ and acceptor absorption $\epsilon_A(\lambda)$ spectra defined by

$$J = \int F_D(\lambda)\, \epsilon_A(\lambda) \lambda^4\, d\lambda / \int F_D(\lambda)\, d\lambda \quad (4)$$

The quantum yield of DNS-actin in buffer G was determined

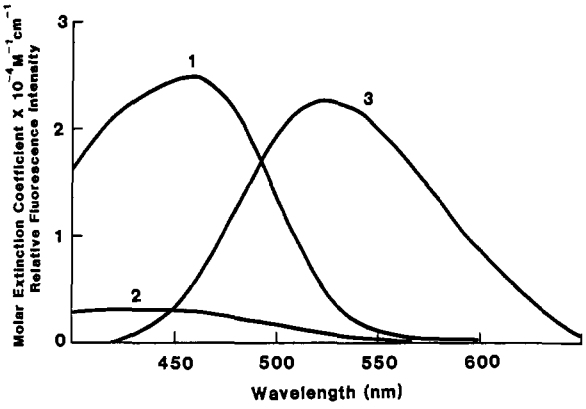

FIGURE 1: Spectral overlap of the absorption spectrum of DABMI (1) or DDPM (2) attached to Cys-374 on actin and the fluorescence spectrum of DNS-Cl attached to Tyr-69 on actin excited at 360 nm (3). Spectra were measured in 2 mM Tris-HCl (pH 8.0)/0.1 mM ATP/0.1 mM $CaCl_2$ at 20 °C.

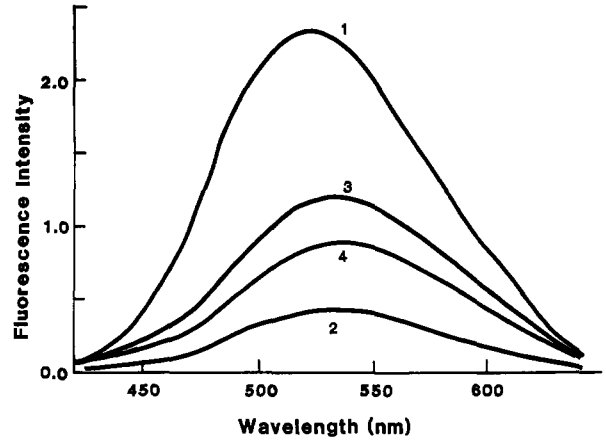

FIGURE 2: Fluorescence spectra of DNS-actin (1), DNS-DABM-actin (2), trypsin-digested DNS-actin (3), and trypsin-digested DNS-DABM-actin (4) at 20 °C. Actin concentration was 0.14 mg/mL in buffer G (1 and 2) or in buffer G + 1% SDS (3 and 4). Excitation wavelength was 360 nm.

to be 0.12, taking the quantum yield of fluorescein in 0.1 M NaOH of 0.85 as the standard (Parker & Reese, 1966). κ^2 was taken as $^2/_3$ for calculation of distances.

Other Methods. Viscosity was measured at 25 °C with an Ostwald viscometer having an outflow time of 52 s for water. DNase I activity was measured by the hyperchromicity assay of Kunitz (1950) at 260 nm and room temperature. The assay used contained 0.05 mg/mL of DNA in 60 mM Tris-HCl (pH 7.5)/2.4 mM $MgCl_2$/1.05 mM $CaCl_2$. SDS–polyacrylamide gel electrophoresis (SDS–PAGE) was carried out according to Laemmli (1970).

Results

Spectral Relation of Donor and Acceptor. Figure 1 shows the emission spectrum of DNS-actin and the absorption spectra of DABMI and DDPM bound to actin. The overlap integral for each donor–acceptor pair was calculated according to eq 4. J was calculated to be 4.16×10^{14} M^{-1} cm^{-1} for DABMI and 6.00×10^{13} M^{-1} cm^{-1} for DDPM. By taking $n = 1.4$, $\kappa^2 = {}^2/_3$, and the quantum yield of DNS-actin as 0.12, Förster's critical distance $R_0(^2/_3)$ was calculated to be 3.02 nm for DABMI and 2.19 nm for DDPM, according to eq 3.

Distance between Tyr-69 and Cys-374 on G-Actin. The resonance energy transfer was measured between DNS-Cl attached to Tyr-69 and DABMI or DDPM attached to Cys-374 on G-actin. The emission spectra of DNS-actin and DNS-DABM-actin excited at 360 nm were measured in buffer G at 20 °C (Figure 2). The concentration of actin was 0.14 mg/mL. The emission peak of DNS-actin was at 523 ± 3 nm. Then, the fluorescence intensities at 520 nm were compared for calculation of the transfer efficiency using eq 1. The fluorescence intensity of DNS-DABM-actin was only 18.4% of that of DNS-actin. This decrease in fluorescence intensity could be attributed mainly to the resonance energy from DNS to DABM on G-actin. However, the fluorescence intensity depends on the concentration of the fluorophore in sample solution. It is difficult to precisely determine the labeling ratio of DNS-Cl to the doubly labeled DNS-DABM-actin, since the absorption of DABM overlaps with that of DNS-Cl. Consequently, it is difficult to adjust the concentrations of the fluorophore in two sample solutions. Moreover, the existence of the acceptor molecule may decrease the fluorescence intensity not only through resonance energy transfer but also through inner-filter effects. From the absorptions at the excitation (A_{ex}) and emission (A_{em}) wavelengths, the decrease of the fluorescence intensity due to inner-filter effects can be estimated by use of the following equation, when a 1×1 cm^2 cuvette is illuminated centrally and observed at a right angle (Lakowicz, 1983; Miki, 1990):

$$F_{obs} = F_{corr}(10^{-(A_{ex}+A_{em})/2}) \quad (5)$$

where F_{obs} and F_{corr} are the observed and correct fluorescence intensities, respectively. In the present case (DNS-DABM-actin), inner-filter effects decrease the fluorescence intensity by about 10% when excited at 360 nm and measured at 520 nm. Therefore, these factors should be taken into account when the transfer efficiency is calculated.

To overcome these difficulties, the following samples were prepared. Trypsin to 0.4 mg/mL was added into the samples (DNS-actin and DNS-DABM-actin) and incubated at 20 °C for 1 day. SDS-PAGE showed that actin was completely digested into small peptides. After digestion, SDS to 1% was added into samples. Then the donor (DNS) and the acceptor (DABM) are separated from each other, and consequently, the resonance energy transfer no longer occurs. The fluorescence intensity of digested DNS-DABM-actin was 74% compared to the intensity of digested control DNS-actin in buffer G + 1% SDS. This difference in fluorescence intensity can be attributed to inner-filter effects and to the difference in donor concentrations between DNS-actin and DNS-DABM-actin. Taking this correction factor (0.74) into account, the ratio of fluorescence intensity of DNS-DABM-actin (F_{DA}) to that of DNS-actin (F_{D0}) was determined to be 0.249 (0.184/0.74). The energy-transfer efficiency was thus calculated to be 0.751. This corresponds to a distance of 2.51 nm.

The emission spectra of DNS-actin and DNS-DDPM-actin excited at 360 nm were also measured at 20 °C. The concentration of actin was 0.12 mg/mL. The emission peak was at 523 ± 3 nm for both samples. The fluorescence intensity of DNS-DDPM-actin was 50.0% of that of DNS-actin in buffer G. After digestion by trypsin (0.4 mg/mL), the fluorescence intensity of DNS-DDPM-actin was 87.0% of that of DNS-actin in buffer G + 1% SDS. The transfer efficiency was calculated to be 0.425, which corresponds to a distance of 2.30 nm. Five separate labeling experiments gave an average value of 2.27 ± 0.04 nm.

Effects of Polymerization, DNase I, S1, and Troponin–Tropomyosin on the Resonance Energy Transfer Efficiency between Probes Attached to Tyr-69 and Cys-374. DNS-actin inhibited the DNA degrading activity of DNase I to the same extent as normal G-actin. Thus the modification of Tyr-69 with DNS-Cl does not impair the interaction of actin with

DNase I. The emission spectra of DNS-actin and DNS-DDPM-actin were measured in buffer G in the presence and absence of DNase I. The concentrations of actin and DNase I were 0.12 mg/mL. The emission maximum of DNS-actin did not change by the addition of DNase I, but the intensity decreased by about 20%. The ratio of the fluorescence intensity of DNS-DDPM-actin to that of DNS-actin in the presence of DNase I was 0.498. Using the correction factor obtained from the digestion by trypsin as described above, the transfer efficiency was calculated to be 0.428. Taking into account the change in quantum yield Q_{D0} (20%), the distance was calculated to be 2.21 nm. The decrease in the distance between in the presence and absence of DNase I was only 0.06 nm.

DNS-actin and DNS-DDPM-actin were polymerized by the addition of a 2-fold molar excess of phalloidin (Miki et al., 1987a). The emission spectra of DNS-actin and DNS-DDPM-actin were measured in 30 mM KCl/20 mM Tris-HCl (pH 7.6)/2 mM $MgCl_2$ (buffer F) in the absence (G-actin) and presence (F-actin) of phalloidin. The concentration of actin was 0.12 mg/mL. The emission peak of DNS-actin did not change after polymerization, but the fluorescence intensity decreased by 14%. The fluorescence intensity of DNS-DDPM-actin at 520 nm was compared with that of DNS-actin in G-actin and in F-actin. In G-actin, the fluorescence intensity of DNS-DDPM-actin was 0.50 of that of DNS-actin, but after polymerization, it was 0.45 of that of DNS-actin. Using the correction factor obtained for the digestion of G-actin by trypsin, the transfer efficiency in F-actin was calculated to be 0.487. Taking into account the change in quantum yield (14%), the distance was calculated to be 2.16 nm, assuming that the energy transfer occurs only between probes in an actin monomer (intramonomer transfer). The distance was shorter by 0.12 nm than that in G-actin.

When the doubly labeled actin monomers polymerize, an additional energy transfer occurs due to intermonomer energy transfer between sites in its neighboring monomers. At the present, it cannot be determined what portion of the change in the transfer efficiency during polymerization is due to this intermonomer energy transfer. However, taking into account a contribution of the intermonomer energy transfer, the change in the transfer efficiency due to the intramonomer distance change should be smaller than the total change during polymerization. Consequently, a decrease in the distance between Tyr-69 and Cys-374 in an actin monomer during polymerization can be calculated to be less than 0.12 nm.

The emission spectra of DNS-F-actin and DNS-DDPM-F-actin in the presence and absence of S1 were measured in buffer F at 20 °C. The concentrations of actin and S1 were 0.12 and 0.35 mg/mL, respectively. The emission spectrum of DNS-F-actin did not change by S1 binding, but the fluorescence intensity decreased by 7%. The ratio of the fluorescence intensity of DNS-DDPM-actin to that of DNS-actin in the presence of S1 was 0.498. The transfer efficiency was calculated to be 0.428, which corresponds to a distance of 2.21 nm. The distance between probes attached to Tyr-69 and Cys-374 in the acto–S1 complex was longer by only 0.05 nm than that in the absence of S1.

The effect of tropomyosin–troponin on DNS-F-actin and DNS-DDPM-F-actin (molar ratio of tropomyosin:troponin:actin = 1:1:7) was measured in buffer F + 0.1 mM $CaCl_2$ (in the presence of Ca^{2+}) or 1 mM EGTA (in the absence of Ca^{2+}). The addition of tropomyosin–troponin to DNS-F-actin and DNS-DDPM-F-actin did not change the fluorescence intensities appreciably (<4%) whether Ca^{2+} was present or not. A change in the distance between Tyr-69 and Cys-374 on an actin monomer in F-actin in the presence and absence of Ca^{2+} is less than 0.1 nm.

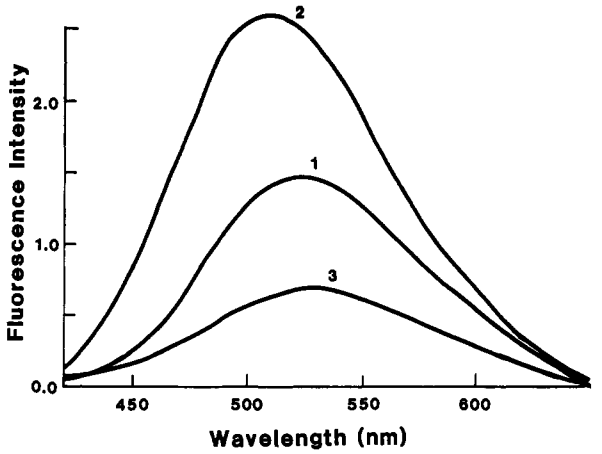

FIGURE 3: Fluorescence spectra of DNS-actin (1), EDTA-denatured DNS-actin (2), and urea-denatured DNS-actin (3) at 20 °C. Actin concentration was 0.14 mg/mL in 0.1 mM ATP/0.1 mM $CaCl_2$/8 mM Tris-HCl (pH 8.0) (buffer A) (1), buffer A + 1 mM EDTA (2), and buffer A + 8 M urea (3). The excitation wavelength was 360 nm.

A Conformational Change at Tyr-69 during Denaturation by EDTA. Once actin is denatured by the addition of EDTA, it does not polymerize even in the presence of phalloidin. The time course of the loss in the polymerizability of DNS-actin was measured after treatment with EDTA. DNS-actin (2 mg/mL) was incubated in 0.1 mM ATP/0.1 mM $CaCl_2$/8 mM Tris-HCl (pH 8.0) (buffer A) + 1 mM EDTA at 20 °C. At time intervals, DNS-actin (1 mg/mL) was polymerized in buffer F + a 2-fold molar excess of phalloidin. After 1-day incubation at room temperature, the viscosities were measured at 20 °C. The half-time for the total loss in the polymerizability of DNS-actin was 40 min. This rate is in good agreement with a previous report which was obtained from circular dichroism measurements of unlabeled G-actin (Strzelecka-Golaszewska et al., 1985).

The emission spectra of DNS-actin in buffer A, in buffer A + 1 mM EDTA, and in buffer A + 8 M urea are shown in Figure 3. The fluorescence intensity of DNS-actin increased by 80%, and a blue shift of the emission peak from 523 ± 3 nm to 506 ± 3 nm was observed following the addition of EDTA. In contrast, in buffer A + 8 M urea, the decrease of the fluorescence intensity by 53% and a red shift (about 7 nm) of the emission peak of DNS-actin were observed. DNS-actin was incubated in buffer A at 75 °C for 1 h. The polymerizability of DNS-actin was completely lost after this treatment. The emission spectrum was measured at 20 °C. A similar increase in the fluorescence intensity and the blue shift in the emission peak of DNS-actin were observed as in the case of EDTA denaturation. The results indicate that dansyl chromophore on both EDTA- and heat-denatured actin is less exposed to solvent than in the native state.

The time course of the fluorescence intensity change of DNS-actin in 8 mM Tris-HCl (pH 8.0)/26 μM $CaCl_2$/26 μM ATP after the addition of EDTA (final concentration 1 mM) was followed at 500 nm and 20 °C (Figure 4). The fluorescence intensity increased very rapidly after the addition of EDTA. The half-time for the fluorescence intensity change was 3.5 min. The addition of ATP (up to 2 mM) decreased the rate of the fluorescence intensity change, but did not inhibit the change. Even in the presence of 2 mM ATP, the fluorescence intensity increased significantly. On the other

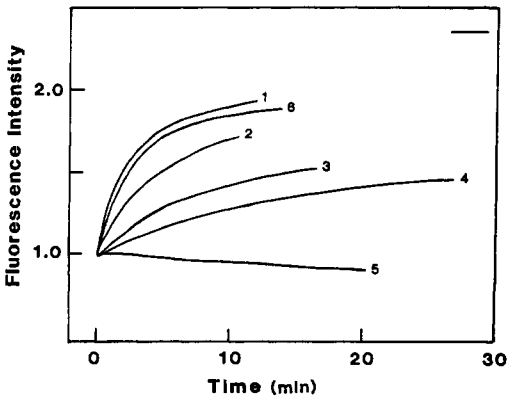

FIGURE 4: Time course of the fluorescence intensity change of DNS-actin after addition of EDTA (1 mM) in 8 mM Tris-HCl (pH 8.0)/26 μM $CaCl_2$ and 26 μM (1), 0.25 mM (2), 1 mM (3), or 2 mM ATP (4), 26 μM ATP + DNase I (5), or 26 μM ATP + S1 (6). Concentrations of DNS-actin, DNase I, and S1 were 0.1, 0.1, and 0.272 mg/mL, respectively. Fluorescence intensity was measured at 500 nm and 20 °C.

hand, the addition of an equimolar amount of DNase I to DNS-actin completely inhibited the increase in fluorescence intensity. The emission spectrum of DNS-actin was not changed by the addition of EDTA even after 2 h in the presence of DNase I. The addition of S1 did not change the fluorescence intensity of DNS-actin, nor did S1 affect the rate of the fluorescence intensity change by EDTA.

Resonance energy transfer between probes attached to Tyr-69 and Cys-374 on actin was measured after denaturation of DNS-actin by 2 mM EDTA and also by 8 M urea. The fluorescence intensity excited at 360 nm was measured at 520 nm at 20 °C. The intensity increased after addition of EDTA as shown in Figure 3. However, the ratio of the fluorescence intensities of DNS-DDPM-actin to DNS-actin did not change significantly. The ratio was 0.484 in 6 mM Tris-HCl (pH 8.0)/0.01 mM ATP/0.01 mM $CaCl_2$, was 0.484 1 h after the addition of EDTA, and saturated to the value of 0.505 after 2 h. Taking into consideration the change in the quantum yield and the emission spectrum of DNS-actin after addition of EDTA, $R_0(^2/_3)$ was calculated to be 2.50 nm. The distance between probes attached to Tyr-69 and Cys-374 was calculated to be 2.64 nm, which is longer by 0.37 nm than that on native G-actin. On the other hand, in the presence of 8 M urea, no energy transfer was observed, suggesting that the distance is greater than 4.0 nm, which is the limiting distance for the present donor–acceptor pair. This is consistent with the evidence that proteins are completely unfolded in 8 M urea, and consequently the donor is too far from the acceptor on the peptide of actin for resonance energy transfer.

Discussion

Intramonomer Distances in G-Actin. The distance between Tyr-69 and Cys-374 was determined to be 2.51 nm using DNS-Cl as a donor and DABMI as the acceptor. This value is significantly smaller than that in a previous report (Barden & dos Remedios, 1987). In the previous studies, after the modification of Cys-374 with DABMI, Tyr-69 was nitrated with tetranitromethane, and then DNS-Cl was reacted with Tyr-69. However, during nitration of Tyr-69 and its amination with sodium tetrathionate, the chromophore of DABMI attached to Cys-374 is bleached, and consequently the absorbance of DABMI on the double-labeled actin (DNS-DABM-actin) is strongly reduced. This causes a decrease in the apparent transfer efficiency, and consequently an increase in the calculated distance.

In this paper, Cys-374 was protected reversibly by the treatment with sodium tetrathionate during the modification of Tyr-69 with DNS-Cl. Then, after deprotection by dithiothreitol, Cys-374 was labeled with DABMI or DDPM. The donor–acceptor pairs DNS-Cl and DABMI or DDPM gave distances of 2.51 and 2.27 nm, respectively. In the atomic model of actin, the distance between the oxygen position of the hydroxyl group of Tyr-69 and the S_γ position of Cys-374 is given as 2.9 nm (Kabsch et al., 1990). On the other hand, fluorescence resonance energy transfer measurements determine the separation of the transition moments of the donor and acceptor moiety rather than the distance between the residue side chains (Tao & Lamkin, 1981). In general, the size of probes ranges from 0.5 to 1.5 nm. Taking into account these considerations, the present result is in good accordance with the X-ray analysis.

The emission spectrum of DNS-DABM-actin was apparently different from that of DNS-actin (spectra 1 and 2 in Figure 2). This difference can be attributed to the inner-filter effects. At shorter wavelengths, more absorption of DABM (Figure 1) contributes to the inner-filter effects (eq 5) and consequently the emission spectrum of DNS-DABM-actin was distorted. On the other hand, the absorption of DDPM is much smaller than that of DABM (Figure 1). Then, the contribution of inner-filter effects is not significant in the case of DNS-DDPM-actin. In fact, the emission spectrum of DNS-DDPM-actin was the same as that of DNS-actin.

The value of $^2/_3$ for κ^2 is based on the assumption that both donor and acceptor molecules rotate freely and rapidly. The time-resolved anisotropy decay measurements showed that the probes attached to actin do not rotate freely and that the motion of the probes attached to actin is in the range from several hundred nanoseconds to several microseconds (Wahl et al., 1975; Miki et al., 1982). In this case, the maximum and minimum boundaries for κ^2 can be calculated using the limiting anisotropies (Dale et al., 1979). The limiting anisotropy of DNS-actin was determined to be 0.281 from the polarization measurements in the temperature range from 10 to 40 °C. The fundamental anisotropy of the DNS moiety was reported to be 0.351 (Kasprzak et al., 1988). These values give an error range for the critical distance R_0 calculated using $\kappa^2 = ^2/_3$ of about ±35%, assuming that the energy acceptor has no rotational freedom. If the extent of the rotational freedom of the acceptor molecule is taken into account, the error range becomes smaller. It should be noted that the maximum and minimum values for κ^2 correspond to the case where the axis of the cone in which the donor and acceptor transition moments rotate rapidly are oriented entirely along unique directions (i.e., perpendicular or parallel). Usually, proteins are not rigid but flexible macromolecules, and the directions of the transition moments of probes may be randomized by segmental motions of proteins in an equilibrium state. Therefore, an actual value for κ^2 is probably very close to $^2/_3$.

Figure 5 shows a model of the spatial relationships between Lys-61, Tyr-69, Cys-374, the adenine moiety of the bound nucleotide, and the bound metal which were determined from fluorescence resonance transfer measurements using $\kappa^2 = ^2/_3$ (Miki & Wahl, 1985; Barden & Miki, 1986; Miki et al., 1987b; Miki & dos Remedios, 1988). This model is in good accordance with the atomic model of actin (Kabsch et al., 1990). Thus the assumption value of $^2/_3$ for κ^2 seems reasonable.

Intermonomer Distances in F-Actin. In the case of the fluorescence resonance energy transfer between Lys-61 and

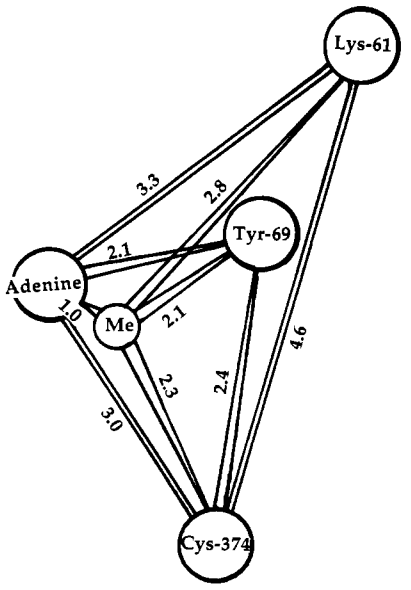

FIGURE 5: A model of the spatial relationships between Lys-61, Tyr-69, Cys-374, the nucleotide binding site, and the metal binding site determined by fluorescence resonance energy transfer measurements. The distances are expressed in nm.

Cys-374, a large increase in the transfer efficiency was observed during polymerization indicating that the intermonomer distance is much closer (<3.3 nm) than the intramonomer distance (4.6 nm) (Miki et al., 1987b). On the other hand, for Tyr-69 and Cys-374, only a small increase in the transfer efficiency was observed. The results indicate that there is no large change in the intramonomer distance during polymerization and also that the intermonomer distance between Tyr-69 and Cys-374 is much longer than R_0. Here we estimate the intermonomer distance between Tyr-69 and Cys-374, assuming that the intramonomer distance between Tyr-69 and Cys-374 does not change during polymerization and that the increase of the transfer efficiency during polymerization is due to an extra energy transfer from Tyr-69 on an actin monomer and Cys-374 on its neighboring actin monomer (intermonomer energy transfer). Analysis of fluorescence resonance energy transfer between a single donor and multiacceptors was described previously (Miki et al., 1987b). The fluorescence intensity (F_{DA}) in the presence of multiacceptors is given by

$$F_{DA} = F_{D0}/[1 + \sum_{i=1}^{2}(R_0/R_i)^6] \quad (6)$$

where F_{D0} is the fluorescence intensity in the absence of acceptor, R_1 is the intramonomer distance, and R_2 is the intermonomer distance. Here R_1 was taken to be 2.27 nm. Then the intermonomer distance R_2 can be calculated to be 2.68 nm. This value is in good agreement with the nearest-neighboring distance of 3.1 nm (Kabsch, personal communication) derived from an atomic model of F-actin (Holmes et al., 1990).

Conformational Changes in Actin. The atomic model of actin locates Tyr-69 and Cys-374 in the same small domain but in different subdomains. Table I sumarizes the distances between Tyr-69 and Cys-374 measured in different states of actin. The present results suggest that the structure of the small domain is substantially rigid. A large-scale hinge movement between two subdomains in the small domain seems not to occur. However, the possibility of a such movement between two domains on actin cannot be excluded. The previous fluorescence resonance energy transfer measurements (Miki et al., 1987b) and present results support the F-actin model presented by Holmes et al. (1990).

Table I

state of actin	$R_0(^2/_3)$ (nm)	E	$R(^2/_3)$ (nm)
monomer/+DNase I	2.11	0.428	2.23
monomer	2.19	0.446	2.27
polymer	2.14	0.487	2.16
polymer/+S1	2.11	0.428	2.22
polymer/Tm-Tn/+Ca	2.14	0.493	2.15
polymer/Tm-Tn/-Ca	2.17	0.540	2.11
denatured by EDTA	2.50	0.505	2.64

EDTA Denaturation. During EDTA or heat denaturation, an appeciable red shift of the intrinsic fluorescence spectrum of actin occurs, indicating increased exposure of Trp to the aqueous environment (Lehrer & Kerwar, 1972; Kuznetsova et al., 1988). In contrast, a large blue shift (17 nm) in the fluorescence spectrum and a strong increase in fluorescence intensity of the dansyl chromophore attached to Tyr-69 on actin were observed during the denaturation. On the other hand, when DNS-G-actin is completely unfolded in 8 M urea or digested into small peptides by trypsin, a red shift (5–10 nm) in the fluorescence maximum of the dansyl chromophore is observed. The results indicate that the environment of dansyl chromophore on actin becomes more hydrophobic during denaturation by EDTA or by high temperature in contrast to the case of tryptophan. The distance between Tyr-69 and Cys-374 did not change drastically during the denaturation by EDTA (0.37 nm). These results suggest that the small-domain structure of actin is largely preserved in this intermediate state, although some helix regions involving tryptophan residues may be partially unfolded.

Lewis et al. (1963) measured the physicochemical properties of native and EDTA-denatured G-actin by viscosity, analytical ultracentrifuge, and ORD. They concluded that the denaturation of actin by EDTA causes a large drop in the effective volume of the native G-actin molecule while largely maintaining its secondary structure. The environment of DNS-Cl attached to Tyr-69 becomes more hydrophobic after denaturation by EDTA, while tryptophan residues become more exposed to the aqueous environment (Lehrer & Kerwar, 1972; Kuznetsova et al., 1988). The atomic model of actin locates Tyr-69 on the side of the small domain of actin facing the cleft containing the nucleotide (Kabsch et al., 1990). The release of the nucleotide may induce a collapse of the pocket for the adenine base which causes a closure of the cleft between two domains of actin. The closure of the cleft prevents the denatured actin from rebinding ATP. Then, the transition from the native form to the EDTA denatured form becomes irreversible. This model for the EDTA denaturation process easily explains both of the marked decrease in the apparent swelling of the native G-actin and the marked increase of the hydrophobicity around Tyr-69 during denaturation. DNase I binding to actin reduced the rate of exchange of actin-bound nucleotide by a factor of about 10, but it does not inhibit the release of actin-bound nucleotide by the addition of EDTA (Mannherz et al., 1980; Polzer et al., 1989). DNase I binds two domains of the actin monomer (Kabsch et al., 1990) and then prevents the closure of the cleft. Thus, DNase I stabilizes the structure of actin even after the release of the bound nucleotide.

ACKNOWLEDGMENTS

I thank Dr. Cristobal G. dos Remedios for his support and Dr. W. Kabsch for providing the atomic coordinates of G-actin and F-actin.

Registry No. DABMI, 87963-80-2; DDPM, 3475-74-9; DNS-Cl, 605-65-2.

REFERENCES

Barden, J. A., & dos Remedios, C. G. (1985) *Eur. J. Biochem. 146*, 5–8.

Barden, J. A., & Miki, M. (1986) *Biochem. Int. 12*, 321–329.

Botts, J., Takashi, R., Torgerson, P., Hozumi, T., Muhlrad, A., Mornet, D., & Morales, M. F. (1984) *Proc. Natl. Acad. Sci. U.S.A. 81*, 2060–2064.

Chantler, P. D., & Gratzer, W. B. (1975) *Eur. J. Biochem. 60*, 67–72.

Cummins, P., & Perry, S. V. (1973) *Biochem. J. 133*, 765–777.

Dale, R. E., Eisinger, J., & Blumberg, W. E. (1979) *Biophys. J. 26*, 161–194.

dos Remedios, C. G., Miki, M., & Barden, J. A. (1987) *J. Muscle Res. Cell Motil. 8*, 97–117.

Ebashi, S., Kodama, A., & Ebashi, F. (1968) *J. Biochem. (Tokyo) 64*, 465–477.

Förster, T. (1948) *Ann. Physik. 2*, 55–75.

Gold, A. H., & Segel, H. L. (1964) *Biochemistry 3*, 778–782.

Goto, K., Takahashi, N., & Murachi, T. (1971) *J. Biochem. (Tokyo) 70*, 157–164.

Holmes, K. C., Popp, D., Gebhard, W., & Kabsch, W. (1990) *Nature 347*, 44–49.

Ishiwata, S., & Fujime, S. (1972) *J. Mol. Biol. 68*, 511–522.

Kabsch, W., Mannherz, H. G., Suck, D., Pai, E. F., & Holmes, K. C. (1990) *Nature 347*, 37–44.

Kasprzak, A. A., Takashi, R., & Morales, M. F. (1988) *Biochemistry 27*, 4512–4522.

Kassab, R., Roustan, C., & Pradel, L.-A. (1968) *Biochim. Biophys. Acta 167*, 308–316.

Kenner, R. A., & Neurath, H. (1971) *Biochemistry 10*, 551–557.

Kunitz, M. (1950) *J. Gen. Physiol. 33*, 349–362.

Kuznetsova, I. M., Khaitlina, S. Yu., Konditerov, S. N., Surin, A. M., & Turoverov, K. K. (1988) *Biophys. Chem. 32*, 73–78.

Laemmli, U. K. (1970) *Nature (London) 227*, 680–685.

Lakowicz, J. R. (1983) *Principles of fluorescence spectroscopy*, Plenum Press, New York.

Lehrer, S. S., & Kerwar, G. (1972) *Biochemistry 11*, 1211–1217.

Lewis, M. S., Maruyama, K., Carroll, D. R., Kominz, D. R., & Laki, K. (1963) *Biochemistry 2*, 34–39.

Liang, P. (1941) *Org. Synth. 21*, 105–107.

Mannherz, H. G., Goody, R., Konrad, M., & Nowak, E. (1980) *Eur. J. Biochem. 104*, 367–379.

Maruyama, K., & Gergely, J. (1961) *Biochem. Biophys. Res. Commun. 6*, 245–249.

Miki, M. (1990) *Eur. J. Biochem. 187*, 155–162.

Miki, M., & Wahl, Ph. (1985) *Biochim. Biophys. Acta 828*, 188–195.

Miki, M., & dos Remedios, C. G. (1988) *J. Biochem. (Tokyo) 104*, 232–235.

Miki, M., Wahl, Ph., & Auchet, J. C. (1982) *Biophys. Chem. 16*, 165–172.

Miki, M., Barden, J. A., dos Remedios, C. G., Phillips, L., & Hambly, B. D. (1987a) *Eur. J. Biochem. 165*, 125–130.

Miki, M., dos Remedios, C. G., & Barden, J. A. (1987b) *Eur. J. Biochem. 168*, 339–345.

Oosawa, F. (1983) in *Muscle and Nonmuscle Motility* (Stracher, A., Ed.) Vol. 1, pp 151–216, Academic Press, New York.

Parker, C. A., & Reese, W. T. (1966) *Analyst 85*, 587–600.

Pihl, A., & Lange, R. (1962) *J. Biol. Chem. 237*, 1356–1362.

Pollard, T. D. (1990) *Curr. Opin. Cell Biol. 2*, 33–40.

Polzer, B., Nowak, E., Goody, R., & Mannherz, H. G. (1989) *Eur. J. Biochem. 182*, 267–275.

Riordan, J. F., & Christen, P. (1968) *Biochemistry 7*, 1525–1530.

Spudich, J. A., & Watt, S. (1971) *J. Biol. Chem. 246*, 4866–4871.

Strzelecka-Golaszewska, H., Venyaminov, S. Yu., Zmorzynski, S., & Mossakowska, M. (1985) *Eur. J. Biochem. 147*, 331–342.

Tao, T., & Lamkin, M. (1981) *Biochemistry 20*, 5051–5055.

Tao, T., Lamkin, M., & Lehrer, S. S. (1983) *Biochemistry 22*, 3059–3066.

Weeds, A. G., & Pope, B. (1977) *J. Mol. Biol. 111*, 129–157.